

## COMPARISON OF EXPERIMENTAL AND NUMERICAL METHODS OF PATIENT DOSE ESTIMATIONS IN CT USING ANTHROPOMORPHIC MODELS

M. L. Fehrmann<sup>a,b</sup>, H. Schlattl<sup>a,\*</sup>, A. Scheegerer<sup>c,d</sup>, T. Werncke<sup>e</sup>

<sup>a</sup>Institute of Radiation Medicine, Helmholtz Zentrum München - German Research Center for Environmental Health, Neuherberg, Germany, <sup>b</sup>Lehrstuhl für Experimentelle Physik IV, Technische Universität Dortmund, Dortmund, Germany, <sup>c</sup>Medizinischer und beruflicher Strahlenschutz, Bundesamt für Strahlenschutz, Neuherberg, Germany, <sup>d</sup>Institut für Radiologie und Nuklearmedizin, Luzerner Kantonsspital, Luzern, Switzerland, <sup>e</sup>Institut für Diagnostische und Interventionelle Radiologie, Medizinische Hochschule Hannover, Hannover, Germany

**The common methods for patient dose estimations in CT are TLD measurements or the usage of software packages based on Monte Carlo simulations like CT-Expo or the newer CTVoxDos, which uses the ICRP Reference Adult Male (ICRP 110). Organ (OD) and effective doses (ED) of a CT protocol of the upper abdomen are compared. Compared to CTVoxDos, organ doses inferred by TLD measurement using an anthropomorphic phantom differ by  $(19 \pm 16) \%$  inside the primary radiation field,  $(14 \pm 2) \%$  for partially primary irradiated organs and  $(34 \pm 38) \%$  in the scattered radiation field. ODs estimated by CT-Expo show a mean deviation of  $(16 \pm 9) \%$  (primary irradiated) and  $(28 \pm 31) \%$  (scatter irradiated) from ODs estimated by CTVoxDos.**

### INTRODUCTION

Since the first clinical computed tomography (CT) examination was conducted by G. N. Hounsfield and J. Ambrose in 1972, the technique has constantly been developed further and became a well established method in medical imaging. Despite its benefits, a CT examination is always accompanied with a radiation exposure of the patient. Although in 2014 only 9% of the radiological examinations in Germany were CT examinations, the contribution of CT examinations on the collective effective dose was 65%<sup>(1)</sup>. The high contribution of CT examinations to the collective effective dose gives reason for the need of an accurate estimation of the protection quantities organ dose (OD) and effective dose (ED) for CT examinations.

The protection quantities can be estimated using either an anthropomorphic model filled with thermoluminescence dosimeters (TLDs) or Monte Carlo (MC) simulations using computational models of the human body. The first anthropomorphic computational model was developed by the Oak Ridge National Laboratory<sup>(2)</sup>. The body and organs in this model are modelled using geometrical forms like cylinders, ellipsoids and cones. From this hermaphrodite model, an adult male (ADAM) and female (EVA) model were developed by Kramer et al.<sup>(3)</sup>. To achieve a more realistic model, so-called voxel models were developed<sup>(4–8)</sup>. Voxel models are computational models based on CT or MRI image data of individuals. Every voxel (volume element) is assigned to a specific organ, tissue or bone. In 2007, the ICRP has introduced a

male (RCP-AM) and female (RCP-AF) adult reference voxel model that were derived from image data of two individuals and adapted to the data of Reference Man according to ICRP Publication 89<sup>(9)</sup>. Several publications have shown that the simplifications of ADAM and EVA have an impact on the estimated organ doses and effective dose<sup>(10–14)</sup>.

To provide an easy way for the estimation of ODs and EDs in CT, computational programs like WinDos, CT-Expo and ImPACT were developed<sup>(15–17)</sup>. But none of these software packages uses the voxel model of Reference Man recommended by the ICRP<sup>(18)</sup>. Therefore, a new software package, called CTVoxDos<sup>1</sup> has been developed at the Helmholtz Zentrum München. CTVoxDos bases on previous publications<sup>(19,20)</sup>, where MC simulations using an EGSnrc V 4-2-3-0<sup>(21)</sup> user code have been performed. Dose estimations of CTVoxDos are based on the volume CT dose index ( $CTDI_{vol}$ ) that has been shown to be a rather scanner-independent dose quantity for organ dose estimations<sup>(22)</sup>.

The given study aims to compare experimental and numerical methods for patient dose estimations in CT. This comprises TLD measurement using an anthropomorphic model (CIRS ATOM 701-C), numerical simulations of a virtual model of this phantom, CTVoxDos with RCP-AM<sup>(18)</sup> and CT-Expo with ADAM<sup>(3)</sup>. Subsequently, the differences of ODs and EDs determined in all the described cases are evaluated.

\*to whom correspondence should be addressed

<sup>1</sup> CTVoxDos can be obtained from the corresponding author freely for non-commercial purposes.

**Table 1. Setting of the CT protocol parameter.**

parameter	
$U$ [kV]	120
$CTDI_{vol}$ [mGy]	15.04
primary radiation field	slice 21 - 30 <sup>a</sup>
DLP [mGy·cm]	360.53
pitch	0.938
$N \cdot h_{col}$ [mm]	16 · 0.625
automatic tube current modulation	no
number of scans	1

<sup>a</sup>The slices are counted from top to bottom.

In this context, the quality of dose estimations using the new software package CTVoxDos is investigated, too.

## MATERIALS AND METHODS

In order to investigate the differences in the dose estimations of a TLD measurement and the software packages CT-Expo and CTVoxDos, ODs and EDs of a CT examination are determined and compared by five different methods:

1. TLD measurement using the CIRS ATOM 701-C dosimetry phantom (ATOM phantom). The TLDs are set according to the CIRS organ map book.
2. MC simulation using a computational model (ATOM model) of the ATOM phantom using single measurement points according to the CIRS organ map book.
3. MC simulation using a computational model of the ATOM phantom using all voxel of an organ (ATOM model)
4. CTVoxDos using the voxel model of the ICRP Reference Male<sup>(18)</sup>
5. CT-Expo using the ADAM model

The CT parameter are listed in Table 1. The scan range corresponds to a CT examination of the upper abdomen. This CT examination was chosen since most of the radiation sensitive organs<sup>(23)</sup> are completely or partially included in the primary radiation field.

### Phantom TLD measurement

The phantom TLD measurement is conducted at a GE BrightSpeed 16 slice CT device (GE Healthcare, Chicago, Illinois, USA) (installed at the Helmholtz Zentrum München) using the CT parameter given in Table 1. The adult male CIRS ATOM 701-C phantom (Computerized Imaging Reference Systems, Inc., Norfolk, Virginia, USA) serves as dosimetry phantom. In the following, this phantom is called

ATOM phantom. It has a total body length of 173 cm and weighs 73 kg<sup>(24)</sup>. It is built of simulated tissue equivalent materials. The phantom consists of 66 slices (39 slices trunk including head and 27 slices legs), each with a thickness of 2.5 cm and an additional foot. Each slice has a grid ( $1.5 \times 1.5 \text{ cm}^2$ ) of drill holes with 5 mm diameter to host the thermoluminescence dosimeters (TLD). The holes are filled with plugs of the corresponding tissue (5 mm diameter, 25 mm height) with and without the prepared TLD (LiF:Mg, TLD-100; Bicon-Harshaw, Cleceland, Ohio, USA) rods ( $1 \times 1 \times 6 \text{ mm}^3$ ) included. The dosimeters are placed according to the manufacturer's organ map book for the CIRS ATOM 701-D published by CIRS (CIRS, Norfolk, Virginia, USA)<sup>(25)</sup> in all slices of the trunk (slice 10-30). The slices are numbered according to the organ map book. In the TLD measurement, the phantom without arms and without legs is used.

The TLD rods are calibrated for absorbed dose in water. For this purpose, a conventional x-ray tube with a tube voltage of 120 kV and a tube current of 10 mA is used. The radiation quality of the CT system is simulated by an additional 5 mm Al filtration. The annealing of the TLD rods is carried out following a standard procedure<sup>(26)</sup>. The uncertainty of the TLD measurements can be estimated with 9% according to Lechel et al.<sup>(27)</sup>.

With the resulting TLD doses (TD) doses in organs and bones (i.e., red bone marrow) are derived according to the organ map book<sup>(25)</sup>. Red bone marrow doses are, however, not considered in this work, since the detailed implementation of red bone marrow dosimetry in the Monte Carlo code could lead to artificial difference that should not be discussed in this work. The effective dose is calculated according to ICRP 103<sup>(23)</sup>.

### Monte Carlo Simulation

#### Simulation Code

The simulation of the CT examination is based on the Monte Carlo simulation code EGSnrc V4-2-3-0<sup>(21)</sup>, which is an improved version of the EGS4 code<sup>(28)</sup>, maintained by the National Research Council of Canada (NRC). EGSnrc is a code for the simulation of coupled electron, positron and photon transport. A detailed description of the physical principles that are taken into consideration in the EGSnrc transport code and their mathematical approximations can be found elsewhere<sup>(21)</sup>.

As x-ray source, a model of the GE BrightSpeed 16 slice CT device is used. The model is created similarly to the "equivalent source" method introduced by Turner et al.<sup>(29)</sup>. In this method, the source model is based on measurements of the half value layer and the bowtie profile (dose profile at the primary radiation field) at a stationary x-ray tube. By way of

contrast, in this work a time-resolved air-kerma measurement with a rotational tube is performed that is then deconvolved to yield corresponding stationary values (similar to Boone<sup>(30)</sup>). From these measurements an "equivalent energy spectrum" and an "equivalent bowtie filter description" are generated. For the estimation of the anode spectrum, the software package SpekCalc is used<sup>(31)</sup>.

For the computation of the organ doses, a user code was used, which was developed at the Helmholtz Zentrum München. This user code has already been used in previous publications<sup>(19,20)</sup> and is base of the program CTVoxDos. In the given study the history of  $2 \times 10^9$  initial photons is followed leading the coefficients of variance of less than  $3 \times 10^{-3}$  for all relevant organ dose coefficients. The cut-off energy is set to 2 keV for photons and to 20 keV for electrons. The energy deposited in every voxel is recorded and divided by the mass, resulting in the dose deposited in every voxel. Furthermore, air-kerma at the rotation axis ( $K_a$ ) is recorded. Dose conversion coefficients  $DCC^{K_a}$  are calculated as dose per air-kerma and converted into dose conversion coefficients normalised to  $CTDI_{vol}$  ( $DCC^{CT}$ ) according to

$$DCC^{CT} = DCC^{K_a} \left( \frac{CTDI_w}{K_a} \right)^{-1} N_R \psi$$

The ratio of the  $CTDI_w$  to air-kerma on the rotation axis ( $K_a$ ) depends on the tube voltage (here 120 kV), the filtration, the collimation ( $h_{col}$ ) and the  $CTDI$  phantom (here body). It is determined by an additional simulation using a model of a body  $CTDI$  phantom resulting in  $\frac{CTDI_w}{K_a} = 0.358$ . The product of the number of rotations  $N_R$  and the pitch  $\psi$  can be calculated according to

$$N_R \psi = \frac{z_u - z_l}{h_{col}}$$

where  $z_u$  is the upper and  $z_l$  is the lower boundary of the scan field (here  $z_u - z_l = 24$  cm) and  $h_{col}$  is the slice thickness (here 10 mm). The resulting ODs and ED are calculated by multiplying the  $DCC^{CT}$  with  $CTDI_{vol}$  of the examination. Individual (simulated) TLD doses are obtained analogously by determining  $DCC^K$  in individual voxels which are at the same position as the TLD rods in the real phantom. In all simulations, the attenuation and scattering by the patient table is implemented.

#### *Voxel model of the ATOM 701-C dosimetry phantom*

Based on photographs of the slices of the ATOM 701-C dosimetry phantom at the Charité (Berlin, Germany), a three dimensional voxel model of the phantom was constructed (ATOM model). The voxels of the ATOM model have a size of 0.95514 mm in x- and y-direction

and 25 mm in z-direction. On the bases of medical text books and expertise, organs have been mapped on each photographic slice at their anatomical positions and shapes allowing to compute mean organ doses.

Altogether, the phantom consists of 66 slices. This results in a total body length of 165 cm. The densities of the simulated tissues are chosen according to ICRP 23<sup>(32)</sup>. A lateral and frontal depiction of the ATOM model is given in Figure 1.

The ATOM model is based on a dosimetry phantom of the same type as used in the TLD measurement. Nevertheless, every CIRS ATOM 701-C phantom is individual causing small differences between ATOM phantom and ATOM model used in this study.

#### **CTVoxDos**

##### *Voxel model RCP-AM*

Various voxel models are implemented in CTVoxDos that are based on medical image data of individuals. In the given study, the voxel model RCP-AM is used. This model was developed by the Task Group on Dose Calculations (DOCAL) of ICRP Committee 2 in collaboration with the Helmholtz Zentrum München- German Research Centre for Environmental Health (formerly: GSF - National Research Centre for Environment and Health) and the International Commission on Radiation Units and Measurements (ICRU).

The model has a length of 176 cm and weighs 73 kg. Altogether, the model consists of 1,946,375 voxel, each with a height of 8.0 mm (slice thickness), and a size of 2.137 mm in x- and y-direction. The model consists of 220 slices plus an additional slice of skin at the top and the bottom of the model. Around 140 organs, tissues and parts of it were segmented. A lateral and frontal depiction of the resulting voxelised bones and organs of RCP-AM is given in Figure 1.

##### *The software package*

CTVoxDos is a software package for the calculation of ODs and EDs of CT examinations developed at the Helmholtz Zentrum München. It is a front-end to the dose coefficients computed previously<sup>(19,20)</sup> by the described user code. As input parameter, the package needs at least  $CTDI_{vol}$  values (corresponding to  $CTDI$  head or body phantoms) and the scan range as input. It was shown by Turner et al.<sup>(22)</sup>, that  $CTDI_{vol}$  can be used for a scanner-independent estimations of organ doses.

For a more refined dose determination at the scan edges, pitch, collimation and spiral or axial scan mode can be specified. For spiral acquisition mode, the overscanning range can also be defined. Furthermore, it can be chosen, whether tube current modulation has been used during the CT examination. All additional settings are turned off in the given study.

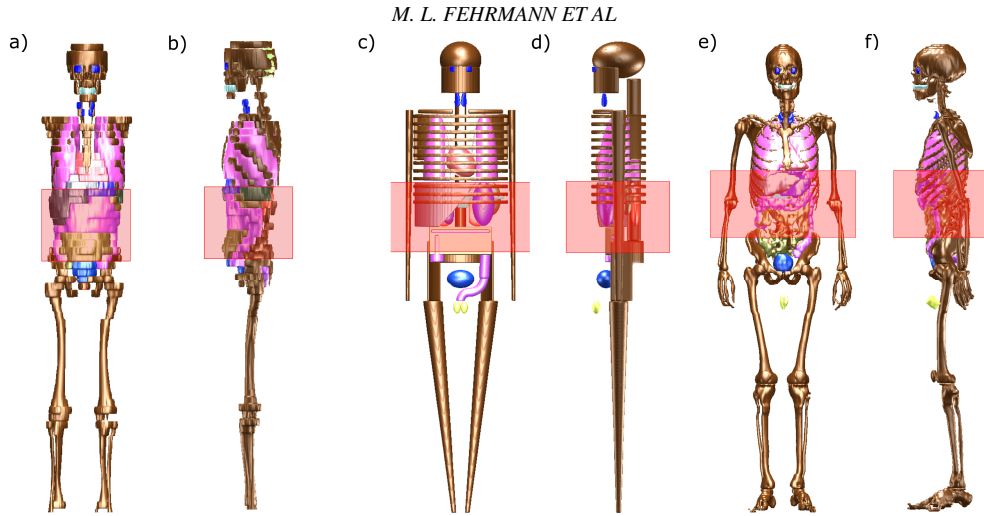


Figure 1. a) Frontal and b) lateral view of the ATOM model, c) frontal and d) lateral view of the ADAM model and e) frontal and f) lateral view of the RCP-AM model with bones and internal organs. The red boxes mark the primary radiation field.

## CT-Expo

### ADAM model

Two adult (ADAM and EVA) and two paediatric (CHILD and BABY) models are implemented in CT-Expo. In the given study, the male adult model called 'ADAM' is used (refer Figure 1). ADAM is a mathematical model that was derived by Kramer et al.<sup>(3)</sup> from the hermaphrodite MIRD-type (Medical Internal Radiation Dose) model (Oak Ridge National Laboratory<sup>(2,18)</sup>, which was the first anthropomorphic computational model. The basis of the models, regarding lengths and masses of the organs and the body, were the data of Reference Man according to ICRP Publication 23<sup>(32)</sup>. The body of the model, as well as its organs, were modelled by the use of geometrical forms, as cylinder, ellipsoids and cones. The main body characteristics of ADAM can be found in<sup>(33)</sup>.

### The software package

CT-Expo is a MS Excel application for the calculation of patient dose quantities that are of interest for the practical use in CT examinations. The software package was developed by Stamm and Nagel in 2001<sup>(16)</sup>. In the given study, CT-Expo Version 2.3.1 (German) is used in the 'calculation' module.

### Definition of scan range

Due to a different organ topology of the various models used in the study: ATOM model, the ATOM phantom, the RCP-AM model and the ADAM model, the scan area is determined using anatomical landmarks. Those

organs that are completely included in the scan area in the CT examination are also included in the scan area of the computational programs and hence primary irradiated. The method of using anatomical landmarks was already used in previous work<sup>(14)</sup>.

Figure 1 shows the scan areas of the different models.

### CTDI measurement

The computed dose quantities depend strongly on the  $CTDI_{vol}$  value. Therefore, the nominal  $CTDI_{vol}$  value given by the CT device is verified by a CTDI measurement with an axial scan using 120 kV, 200 mA, a collimation of 10 mm and a scan time of 4s. This resulted in a nominal  $CTDI_{vol}$  of 89.91 mGy.

### Comparison of the different methods

The comparison of the TLD measurement and CTVoxDos is conducted stepwise by the five different methods. The procedure is outlined in Figure 2. As measure for the comparison, the deviation  $\Delta D^{1,2}$  is computed according to

$$\Delta D^{1,2} = 100 \frac{D_1 - D_2}{D_2}, \quad (1)$$

where  $D$  is either TD, OD or ED.

Initially, the MC simulation on which CTVoxDos is based on is compared with the TLD measurement without the influence of differences in the used dosimetry phantom and computational model ( $\Delta TD^{MC,MEAS}$ ). In the second step, the impact of using only selected points for dose calculations in the TLD measurement is investigated. Therefore ODs are

## COMPARISON OF CT DOSE ESTIMATION METHODS

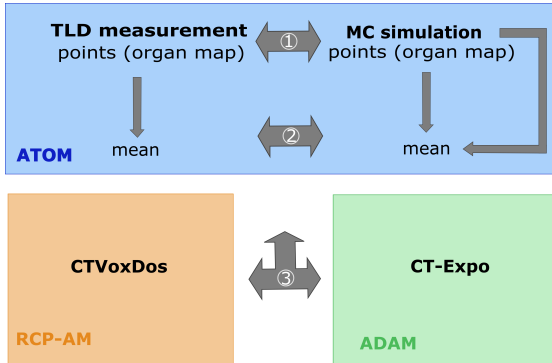


Figure 2. Schematic illustration of the different level of comparison (numbers). The coloured boxes contain calculations that are based on the same anthropomorphic model.

computed by the mean of all measured and computed TDs belonging to a specific organ ( $OD_{pt}$ ). Then, the computed  $OD_{pt}^{MC}$  are compared with  $OD_{mean}$ , i.e., the mean dose of all voxels belonging to the regarded organ.

The third step is to investigate the impact of the different models on the resulting ODs. Therefore, the computed ODs of the organs that are located in the evaluation area are compared. The organ doses are computed by the MC simulation as mean of all voxel using the ATOM model ( $OD_{mean}$ ), CT-Expo using the ADAM model ( $OD^{Expo}$ ) and CTVoxDos using the RCP-AM model ( $OD_{CTVox}$ ). For the comparison, the deviation  $\Delta OD^{i,CTVox}$  of ODs of case  $i$  from  $OD_{CTVox}$  is estimated. Finally, the effective doses resulting from the TLD measurement and the different computations are compared. Therefore, the deviation  $\Delta ED^{i,CTVox}$  of case  $i$  from  $ED_{CTVox}$  is calculated.

## RESULTS

### CTDI measurement

The CTDI measurements yielded  $CTDI_{vol} = (79.38 \pm 0.30)$  mGy, i.e.,  $0.884 \pm 0.003$  times the nominal value. This is within the uncertainty of  $\pm 15\%$  given in the technical reference manual of the GE BrightSpeed 16 device. The factor  $0.884 \pm 0.003$  is used to correct the  $CTDI_{vol}$  of the TLD measurement scan yielding  $(13.28 \pm 0.05)$  mGy. This value is used in the following to obtain TDs, ODs and EDs by the MC simulation and CTVoxDos.

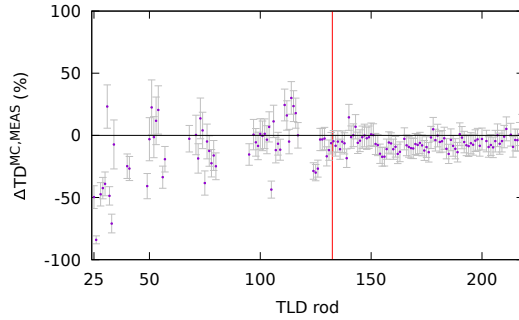


Figure 3. Deviation  $\Delta TD^{MC,MEAS}$  in percent of the computed  $TD^{MC}$  from the measured  $TD^{MEAS}$  for all TLD rods that are located in the evaluation area (slice 10 to 30) and assigned to organs (according to the organ map book<sup>(25)</sup>). TLDs in the primary irradiated area are right of the vertical red line (rod 133 - rod 218).

### Comparison of MC simulation and TLD measurement

#### Single TLD rod doses

Figure 3 shows the comparison of single TLD rod doses of a CT examination of the upper abdomen estimated by the TLD measurement ( $TD^{MEAS}$ ) and the MC simulation ( $TD^{MC}$ ). Only TLD rods of organs (without bones) located in the evaluation area are regarded. Altogether, 144 TLD rods are compared.

In the primary irradiated area,  $|\Delta TD^{MC,MEAS}|$  ranges from  $(0 \pm 9)\%$  (rod 147) to  $(18 \pm 7)\%$  (rod 139). The average  $|\Delta TD^{MC,MEAS}|$  is  $(7 \pm 4)\%$  (with a mean uncertainty of 8%). In the scattered radiation field,  $|\Delta TD^{MC,MEAS}|$  ranges from  $(0 \pm 10)\%$  (rod 117) to  $(84 \pm 3)\%$  (rod 26) with a mean absolute deviation of  $|\Delta TD^{MC,MEAS}| = (19 \pm 18)\%$  (with a mean uncertainty of 11%).

$\Delta TD^{MC,MEAS}$  of the primary and scatter area are  $(-6 \pm 6)\%$  and  $(-12 \pm 23)\%$ , respectively, i.e., tend to be somewhat lower than those of the measurement, and the absolute deviations are increasing with increasing distance to the primary irradiated area.

#### TLD rod organ doses

The ODs estimated from the measured ( $OD_{pt}^{MEAS}$ ) and computed TLD rod doses ( $OD_{pt}^{MC}$ ) are shown in Figure 4. Figure 5 shows the deviation  $\Delta OD_{pt}^{MC,MEAS}$ . Compared to single TDs, a small decrease of the deviation between MC simulation and TLD measurement can be observed for ODs. The deviation  $\Delta OD_{pt}^{MC,MEAS}$  for organs that are completely primary irradiated (stomach, spleen, pancreas, adrenals, gall bladder and kidneys) ranges between  $(-2 \pm 3)\%$

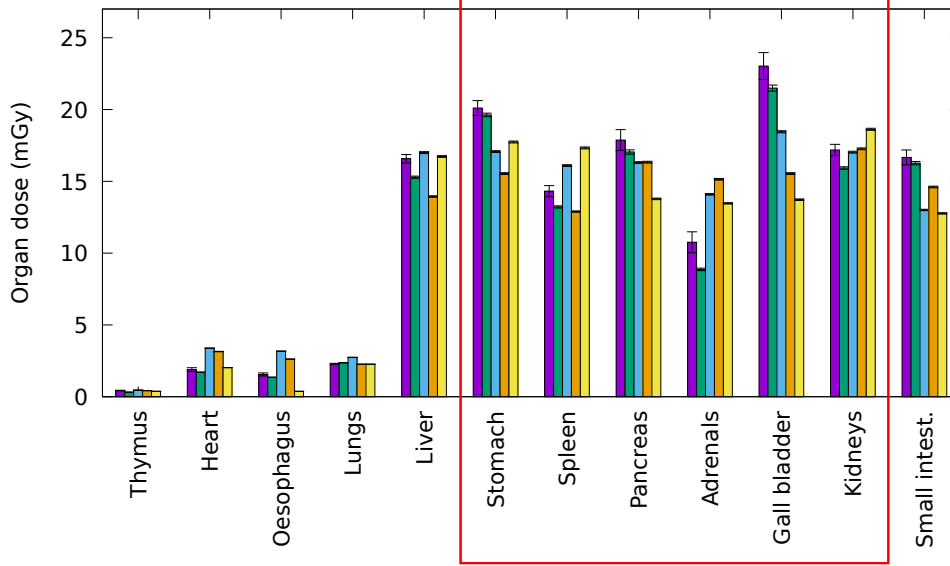


Figure 4. Organ doses in mGy determined for a CT examination of the upper abdomen using different methods (from left to right): purple: TLD measurement (ATOM phantom); green: MC simulation using selected points according to the organ map book<sup>(25)</sup> (ATOM model); light-blue: MC simulation using all voxel of an organ (ATOM model); orange: CTVoxDos (RCP-AM); yellow: CT-Expo (ADAM).

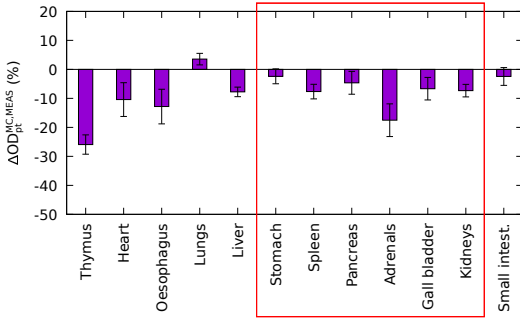


Figure 5.  $\Delta OD_{pt}^{MC,MEAS}$ , the deviation of ODs using selected points according to the organ map book<sup>(25)</sup> between MC simulation (ATOM model) and TLD measurement (ATOM phantom). The red box marks those organs that are completely primary irradiated.

(stomach) and  $(-17 \pm 6) \%$  (adrenals) with a mean  $|\Delta OD_{pt}^{MC,MEAS}|$  of  $(8 \pm 5) \%$  (mean uncertainty: 3%). Organs partially located in the primary radiation field and partially in the scattered radiation are liver and small intestine with  $\Delta OD_{pt}^{MC,MEAS} = (-8 \pm 2) \%$  and  $(-2 \pm 3) \%$ , respectively.

For organs that are completely located in the scatter-irradiated area (thymus, heart, oesophagus and lungs),

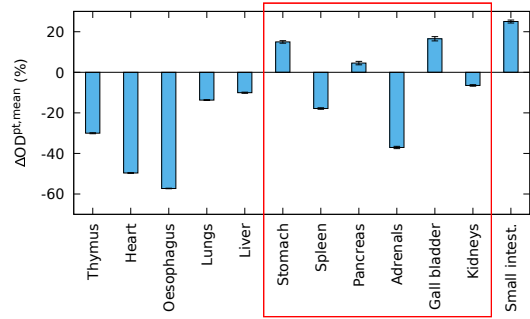


Figure 6.  $\Delta OD_{pt,mean}^{pt,mean}$ , the deviation of ODs (MC simulation, ATOM model) using selected points according to the organ map book<sup>(25)</sup> ( $OD_{pt}$ ) from those using every voxel of an organ ( $OD_{mean}$ ). The red box marks those organs that are completely primary irradiated.

$\Delta OD_{pt}^{MC,MEAS}$  ranges between  $(4 \pm 2) \%$  (lungs) and  $(-26 \pm 3) \%$  (thymus) with a mean  $|\Delta OD_{pt}^{MC,MEAS}|$  of  $(13 \pm 9) \%$  (mean uncertainty: 4%).

#### ODs estimated for single measurement points and all voxel of an organ

The ODs computed by the MC simulation using all voxel that belong to an organ ( $OD_{mean}$ ) are shown

## COMPARISON OF CT DOSE ESTIMATION METHODS

in Figure 4. Figure 6 shows the deviation of  $OD_{\text{mean}}$  from  $OD_{\text{pt}}^{\text{MC}}$  ( $\Delta OD_{\text{pt,mean}}^{\text{MC}}$ ). The uncertainties are here solely given by the statistical uncertainties from the Monte Carlo simulations, because  $CTDI_{\text{vol}}$  cancels in Eq. 1. Organs completely located in the primary radiation field show on average a smaller deviation than organs in the scatter radiation area. In the primary radiation field  $\Delta OD_{\text{pt,mean}}^{\text{MC}}$  ranges between  $(4.5 \pm 0.7)\%$  (pancreas) and  $(37.1 \pm 0.8)\%$  (adrenals) with a mean  $|\Delta OD_{\text{pt,mean}}^{\text{MC}}|$  of  $(16 \pm 12)\%$  (mean uncertainty: 0.5%). Regarding partially primary irradiated organs,  $\Delta OD_{\text{pt,mean}}^{\text{MC}}$  ranges between  $(-10.1 \pm 0.2)\%$  (liver) and  $(25.0 \pm 0.6)\%$  (small intestine). For completely scatter-irradiated organs, the highest values for  $\Delta OD_{\text{pt,mean}}^{\text{MC}}$  can be found. It ranges between  $(-14 \pm 1)\%$  (lungs) and  $(-57 \pm 1)\%$  (oesophagus) with a mean  $|\Delta OD_{\text{pt,mean}}^{\text{MC}}|$  of  $(38 \pm 20)\%$  (mean uncertainty: 2%).

### Comparison of ODs estimated by different models or software packages

#### ATOM model versus RCP-AM (CTVoxDos)

The ODs computed by CTVoxDos using the RCP-AM model ( $OD_{\text{CTVox}}$ ) are shown in Figure 4. Figure 7 shows the deviation of  $OD_{\text{mean}}$  from  $OD_{\text{CTVox}}$ . It shows, that the ODs computed using the ATOM model are mostly greater than the ODs estimated using the RCP-AM model. In the primary irradiated area of RCP-AM, the deviation of ODs estimated using the ATOM model from ODs estimated using the RCP-AM model ( $\Delta OD_{\text{mean,CTVox}}$ ) ranges between  $-0.2\%$  (pancreas) and  $25\%$  (spleen) with a mean  $|\Delta OD_{\text{mean,CTVox}}|$  of  $(10 \pm 10)\%$ . Liver and small intestine, partially primary irradiated in both models, exhibits  $\Delta OD_{\text{mean,CTVox}} = 22\%$  and  $-11\%$ , respectively. For completely scatter-irradiated organs  $\Delta OD_{\text{MC,Vox}}$  ranges between  $7\%$

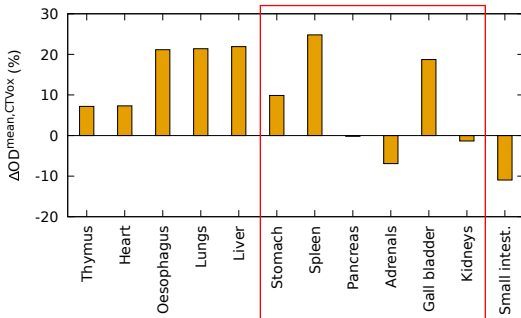


Figure 7.  $\Delta OD_{\text{mean,CTVox}}$ , the deviation of ODs estimated by the MC simulation with the ATOM model<sup>(25)</sup> ( $OD_{\text{mean}}$ ) from those obtained by CTVoxDos with RCP-AM ( $OD_{\text{CTVox}}$ ). The red box marks those organs that are completely primary irradiated.

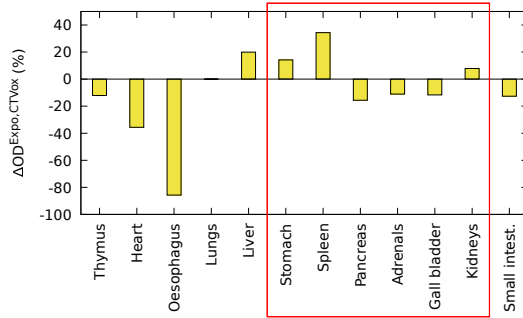


Figure 8.  $\Delta OD_{\text{Expo,CTVox}}$ , the deviation of ODs computed by CT-Expo with the ADAM model<sup>(25)</sup> ( $OD_{\text{Expo}}$ ) from the ODs obtained by CTVoxDos using RCP-AM ( $OD_{\text{CTVox}}$ ). The red box marks those organs that are completely primary irradiated.

(thymus) and  $-21\%$  (lungs and oesophagus) with  $|\Delta OD_{\text{mean,CTVox}}|$  being  $(14 \pm 8)\%$ .

#### CT-Expo versus CTVoxDos

The ODs computed by CT-Expo using the ADAM model ( $OD_{\text{CTVox}}$ ) are shown in Figure 4. Figure 8 shows the deviation of  $OD_{\text{Expo}}$  from  $OD_{\text{CTVox}}$  ( $\Delta OD_{\text{Expo,CTVox}}$ ). In the primary irradiated area,  $\Delta OD_{\text{Expo,CTVox}}$  ranges between  $8\%$  (kidneys) and  $34\%$  (spleen) with a mean of  $|\Delta OD_{\text{Expo,CTVox}}|$  of  $(16 \pm 8)\%$ . Liver and small intestine are partially primary irradiated in CTVoxDos and CT-Expo yielding  $\Delta OD_{\text{Expo,CTVox}} = 20\%$  and  $-13\%$ , respectively. For completely scatter-irradiated organs,  $\Delta OD_{\text{Expo,CTVox}}$  ranges between  $0.01\%$  (lungs) and  $-86\%$  (oesophagus) with  $|\Delta OD_{\text{mean,CTVox}}|$  being  $(33 \pm 38)\%$ .

### Effective doses

The resulting effective dose from TLD measurement, MC simulation, CTVoxDos and CT-Expo and their deviation from CTVoxDos ( $\Delta ED_{\text{CTVox}}$ ) are listed in Table 2. The differences in the EDs are only small compared to the differences in single ODs.

### DISCUSSION

In this study, TDs, ODs and EDs are estimated and compared for only one specific CT examination (upper abdomen). Further investigations of dose estimations for different CT examinations are necessary to better quantify the differences between TLD measurement using the ATOM phantom, CTVoxDos using RCP-AM and CT-Expo using the ADAM model. Nevertheless, the resulting TDs, ODs and EDs give first indications for the

**Table 2. Comparison of EDs of a CT protocol of the upper abdomen determined using a TLD measurement, MC simulation, CT-Expo and CTVoxDos. The effective doses are determined according to ICRP 103<sup>(23)</sup>. Additionally, the deviation (according to equation (1)) of the effective doses from the effective dose determined by CTVoxDos ( $\Delta ED^{i,CTVox}$ ) are listed.**

Method ( <i>i</i> )	ED [mSv]	$\Delta ED^{i,CTVox}$ [%]
TLD	$6.26 \pm 0.07$	$-2 \pm 1$
MC (all voxel)	$6.25 \pm 0.02$	-2
CT-Expo	$5.77 \pm 0.02$	-10
CTVoxDos	$6.4 \pm 0.02$	-

reason and the range of the differences in the estimated dose quantities.

### Comparison of MC simulation and TLD measurement

The comparison of  $TD^{MEAS}$  and  $TD^{MC}$  shows differences between the TLD measurement and the MC simulation when the same measurement positions are used in the ATOM phantom and ATOM model. The agreement is overall good, particularly in the primary irradiated area, although  $TD^{MEAS}$  tend to be somewhat larger than  $TD^{MC}$ . Since ATOM phantom and ATOM model agree in their outer dimensions and the skeletons are similar, it is improbable that the trend is caused by model-phantom differences. It is more likely that the actual  $CTDI_{vol}$  of the scan is somewhat higher than assumed.

### Measured and simulated ODs of ATOM

The difference between  $OD_{pt}^{MEAS}$  and  $OD_{mean}$  is caused by two aspects, the usage of only a limited number of TLDs in the measurements and small differences between ATOM phantom and model in organ topology and bone structure. The differences in ODs between  $OD_{pt}^{MEAS}$  and  $OD_{pt}^{MC}$  (Fig. 5) are mainly caused by the second aspect.

Although the phantom used as basis for the construction of the ATOM model was the same type as in the TLD measurement, both models show small differences in their organ topology and bone structure. These differences have an impact on the computed organ doses which manifests in  $\Delta OD^{pt,mean}$  particularly for organs that are located outside or the edge of the primary irradiated area. The adrenals of the ATOM model are fully within the primary field, but according to the organ map book of the employed ATOM phantom, one of the two adrenals TLDs is in slice 20. Since only a small portion of this slice is within the primary irradiated area, the adrenals dose estimated by TLD is substantially smaller than in the ATOM model ( $\Delta OD^{pt,mean} = -37\%$ ). Similarly, the spleen organ map points are not

all primary irradiated in the TLD measurement but the spleen of the model is completely within the primary irradiated area. But since only 2 of 12 spleen TLDs are outside the primary irradiated area the resulting  $\Delta OD^{pt,mean}$  is smaller than for the adrenals (cf. Fig. 4).

The heart and oesophagus are completely scatter irradiated and show also a clearly higher  $|\Delta OD^{pt,mean}|$  of 50 and 57 %, respectively, than the other scatter-irradiated organs (lungs and thymus). Heart and oesophagus TLDs closest to the primary irradiated area are in slices 18 and 19, respectively, while in the ATOM model these organs extend to slices 20 and 21, respectively, i.e., close to or even within the primary irradiated area. Hence, heart and oesophagus achieve higher doses when all voxel are regarded.

Also for primary irradiated organs, differences in the models are reflected in the resulting ODs. The gall bladder, for example, shows a deviation of  $\Delta OD^{pt,mean} = 17\%$ , since in the ATOM model the gall bladder is located more cranially by one slice than in the ATOM phantom organ map. By this, part of the gall bladder in the model is behind the ribs leading to a lower dose than in the measurement. Moreover, the TLD positions are closer to the body surface further increasing the exposure in antero-posterior direction in the measurements compared to the model simulations.

The stomach is in the model completely behind the ribs, while the organ map book assigns additional TLDs to the stomach in the next two lower slices leading to  $\Delta OD^{pt,mean}$  of 15 %.

### ODs estimated by different models or software packages.

Overall 3 different models are used for the computation of organ doses, ATOM model, RCP-AM (CTVoxDos) and ADAM (CT-Expo). Since in all models the organs are located somewhat differently, dose differences between the models are to be expected. The influence of different organ locations in RCP-AM (and its predecessor Golem) and ADAM for idealised geometries are evaluated previous publications<sup>(10,34)</sup>. Especially the findings for the idealised rotational geometry can be transferred also to CT examinations, and are not all discussed here. The dose difference for organs in the primary field can be summarised to be caused by different positioning in the transverse plane and the smaller antero-posterior abdomen diameter of ADAM. For organs in the scatter-irradiated region, the cranio-caudal position, and thus the distance to the primary field edge is crucially determining the dose. Both effects influence the doses of organs in the partially primary irradiated area.

In the following, only selected special cases are discussed.



## COMPARISON OF CT DOSE ESTIMATION METHODS

### ATOM model versus RCP-AM

In the ATOM model, arms are not included but are present in RCP-AM. This results in a higher shielding against lateral radiation resulting in smaller ODs of RCP-AM in the primary radiation field.

As an example for an organ in the primary irradiated region, the gall bladder OD of the ATOM model deviates by 18 % from the organ dose resulting from CTVoxDos (Fig. 7). In the ATOM model, the gall bladder has a more superficial position compared to RCP-AM. This positioning results in a lower shielding by the trunk and hence a higher dose.

An organ partially primary irradiated is the liver. In the ATOM model, the liver is more caudally located than in RCP-AM. Therefore, a larger portion of ATOM's liver is in the primary irradiated area and it is less shielded by its ribs. This results in a higher liver dose in the ATOM model ( $\Delta OD^{\text{mean,CTVox}} = 22\%$ ).

In the scatter-irradiated area, the oesophagus and lungs show the highest deviation  $\Delta OD^{\text{mean,CTVox}}$  of 21 %. This is caused by a larger portion of these organs being in the primary irradiated area in the ATOM model compared to RCP-AM.

### CT-Expo versus CTVoxDos

Comparing ODs estimated by CT-Expo and CTVoxDos, the greatest difference in the primary irradiated area can be observed for the spleen. This can be explained by a more posterior position in the ADAM model compared to RCP-AM (and its predecessor Golem)<sup>(10)</sup>. Together with the artificial elliptical shape of the trunk in the ADAM model with its smaller back-to-front distance, this leads to higher CT-Expo than CTVoxDos doses (Fig. 8).

The largest deviation of all organs is observed for the oesophagus. In ADAM, the oesophagus is completely outside the primary irradiation area being only exposed to scatter radiation. In RCP-AM a small portion is within the primary irradiated area leading to a substantially higher oesophagus dose.

Besides, different Monte Carlo codes have been used to build the databases of CT-Expo and CTVoxDos. While CTVoxDos is based on EGSnrc<sup>(21)</sup>, for CT-Expo a code developed at Helmholtz Zentrum München has been employed<sup>(33)</sup>. Difference in photon cross sections and the usage of kerma approximation in the latter code leads to further small differences in the doses (cf. eg. Ref.<sup>(34)</sup>).

### Effective doses

The estimated EDs show small differences between the different methods compared to the estimated ODs. Main reason for this is the weighting of the organ doses. According to ICRP 103<sup>(23)</sup>, most of the primary and

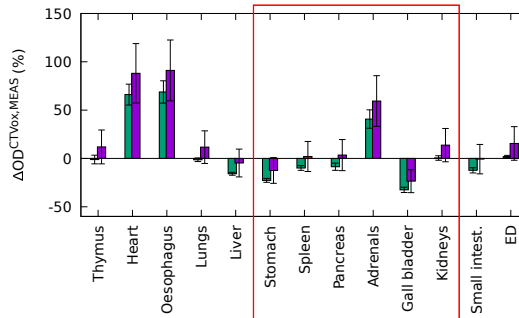


Figure 9.  $\Delta OD^{\text{CTVox,MEAS}}$  and  $\Delta ED^{\text{CTVox,MEAS}}$  computed with (green) and without (purple) a corrected  $CTDI_{\text{vol}}$  value. The red boxes show the primary radiation field. Only organs that are completely located in the evaluation area are shown.

partially primary irradiated organs count as 'remainder'. Therefore, those organs only have a small impact on the effective dose. Scatter irradiated organs with a small organ dose like lungs, thymus and heart have a higher impact on the effective dose. Since the absolute differences between the doses of scatter irradiated organs are only small, the resulting effective doses exhibit only small differences. For other CT protocols, the differences in the EDs might be higher.

### Influence of the corrected $CTDI_{\text{vol}}$ value

CTVoxDos (and CTExpo) is compared with the TLD measurement using a corrected  $CTDI_{\text{vol}}$  value. This is not a standard procedure for OD estimations. Due to the additional expenditure, the  $CTDI_{\text{vol}}$  value given by the CT device is used in general. As an example,  $\Delta OD^{\text{CTVox,MEAS}}$  have been computed with and without a corrected  $CTDI_{\text{vol}}$  value shown in Figure 9. Note, for the uncorrected case, an uncertainty of 15% is assumed for  $CTDI_{\text{vol}}$  according to the technical reference manual of GE. Without the correction, the deviation of the ODs computed by CTVoxDos from the measured ODs ranges from  $(-0.7 \pm 15.2)\%$  (small intestine) to  $(91 \pm 31)\%$  (oesophagus). With the  $CTDI_{\text{vol}}$  correction, the deviation ranges from  $(0.4 \pm 2.3)\%$  (kidneys) to  $(68 \pm 12)\%$  (oesophagus). Although for 50% of the organs the correction leads to an increase of  $\Delta OD^{\text{CTVox,MEAS}}$ , the deviation of the effective dose (ED) decreases from  $(15 \pm 17)\%$  to  $(2 \pm 1)\%$ . Hence, it is concluded that overall a better agreement between CTVoxDos and the measurements was achieved by using the corrected  $CTDI_{\text{vol}}$ .

### CONCLUSION

In this work, the commonly used methods for patient dose estimations in CT: TLD measurements and CT-Expo are compared with simulations and different

software packages, CT-Expo and CTVoxDos. For this purpose, organ doses of selected organs and the effective dose were estimated for a CT protocol of the upper abdomen and compared stepwise.

Initially, the MC simulation on which CTVoxDos is based was verified without the influence of differences in the anthropomorphic models. Single TLD rod doses were measured and computed. The comparison showed a deviation of the MC simulation from the TLD measurement of  $(7 \pm 4 \%)$  inside and  $(19 \pm 18 \%)$  outside of the primary irradiated area. When organ doses are estimated, the deviation is similar for organs that are completely primary irradiated ( $(8 \pm 5 \%)$ ), but smaller for organs that are only partially primary irradiated ( $(5 \pm 4 \%)$ ) or completely scatter irradiated ( $(13 \pm 9 \%)$ ). The MC code of CTVoxDos could therefore be validated for CT dose estimations but the given deviations from the TLD measurement have to be taken into consideration as uncertainty by the evaluation of the computed organ doses.

The influence of various differences in the estimation of CT organ doses by measurements and simulations are quantified. The comparison of organ doses estimated based on single measurement points and all voxel of an organ showed a deviation of  $(16 \pm 12 \%)$  for organs that are completely primary irradiated,  $(18 \pm 11 \%)$  for organs that are only partially primary irradiated and  $(38 \pm 20 \%)$  for organs that are completely scatter irradiated. These deviations give the uncertainty of organ doses estimated from single reference points based on the Atom 701-D organ map book<sup>(25)</sup>. They can only be regarded as guideline, since the stated deviations are still influenced by small differences in the used model and phantom.

Altogether, the mean deviation of organ doses by TLD measurement with the CIRS ATOM 701-C dosimetry phantom (CIRS, Norfolk) ( $OD_{pt}^{MEAS}$ ) from those of simulations using the ATOM model ( $OD_{mean}$ ) can be estimated with  $(15 \pm 9 \%)$  for completely primary irradiated organs,  $(15 \pm 18 \%)$  for partially primary irradiated organs and  $(29 \pm 22 \%)$  for completely scatter irradiated organs. Especially the uncertainties for partially or completely scatter-irradiated organs are only valid for dose estimations for similar CT protocols as in the given study (upper abdomen) due to the strong dependence of the deviations on the distance of the organ to the primary radiation field. Furthermore, it has to be taken into consideration that only selected organs were regarded and the dose quantities were only estimated for a single CT protocol. For a more precise estimation of the uncertainty, further comparisons of dose quantities of different CT protocols are necessary.

The deviation of using the ATOM model instead of RCP-AM ( $\Delta OD_{mean,CTVox}$ ) was estimated with  $(10 \pm 10 \%)$  for organs completely located in the primary irradiated area,  $(16 \pm 8 \%)$  for partially primary irradiated organs and  $(14 \pm 8 \%)$  in case of organs

that are completely scatter irradiated. Inside the primary irradiated area, deviations are mainly caused by the missing shielding of the arms (spleen and kidneys) in case of the ATOM model and a different positioning of the organs inside the trunk.

Doses of organs in the primary irradiated area estimated by CT-Expo deviate absolutely by  $(16 \pm 9 \%)$  from ODs estimated by CTVoxDos. For (partially and fully) scatter-irradiated organs, a mean absolute deviation of  $(28 \pm 31 \%)$  of CT-Expo from CTVoxDos was observed.

Regarding the effective dose, the differences between the various estimations decrease strongly. The deviation of EDs estimated by the TLD measurement, the MC simulation using the ATOM model and CT-Expo from the ED estimated by CTVoxDos range between  $-2 \%$  and  $-10 \%$ , i.e., CTVoxDos estimates the highest effective dose. Noticable, despite the anatomical differences between the ATOM phantom and the IRCP reference male phantom RCP-AM, the effective doses agree with  $(2 \pm 1 \%)$ , when accounting for the correct  $CTDI_{vol}$ -value.

In summary, with respect to the effective dose, all examined methods lead to the same result within a few percent, so can be used as reliable dose estimator.

#### ACKNOWLEDGEMENT

The authors want to thank Ursula Lechel (Bundesamt für Strahlenschutz) for supplying the ATOM phantom and the support by the TLD measurement.

#### REFERENCES

1. Bundesamt für Strahlenschutz. *Umweltradioaktivität und Strahlenbelastung*. Jahresbericht 2015. IV Strahlenexposition durch medizinische Maßnahmen (2016)
2. Fisher, H. L. and Snyder W. S., *Distribution of Dose in the Body from a Source of Gamma Rays Distributed Uniformly in an Organ*. ORNL-4168. Oak Ridge National Laboratory (1967)
3. Kramer, R., Zankl, M. and Williams, G. *The Calculation of Dose from External Photon Exposure Using Reference Human Phantoms and Monte Carlo Methods. Part I: The Male (ADAM) and Female (EVA) Adult Mathematical Phantoms*. GSF-Report S-885. GSF - National Research Center for Environment and Health (1982)
4. Zankl, M., Veit R. and Williams, G. *The construction of computer tomographic phantoms and their application in radiology and radiation protection*. Radiat. Environ. Biophys. **27**, 153–164 (1988)

COMPARISON OF CT DOSE ESTIMATION METHODS

5. Zubal, I. G., Harrell, C. R., Smith, E. O., Rattner, Z., Gindi, G. and Hofer, P. B. *Computerized three-dimensional segmented human anatomy*. Med. Phys. **21**, 299–302 (1994)
6. Xu, X. G., Chao T. C. and Boskurt, A. *VIP-MAN: an image-based whole-body adult male model constructed from color photographs of the Visible Human Project for multi-particle Monte Carlo calculations*. Med. Phys. **78**, 476–486 (2000)
7. Zankl, M. and Wittmann, A. *The adult male voxel model 'Golem' segmented from whole body CT patient data*. Radiat. Environ. Biophys. **40**, 153–162 (2001)
8. Petoussi-Hens, N., Zankl, M., Fill, U. and Regulla, D. *The GSF family of voxel phantoms*. Phys. Med. Biol. **47**, 89–106 (2002)
9. International Commission on Radiological Protection. *Basic Anatomical and Physiological Data for use in Radiological Protection*. ICRP Publication 89, Annals ICRP 32 (3-4) (2002)
10. Zankl, M., Fill, U., Petoussi-Hens, N. and Regulla, D. *Organ dose conversion coefficients for external photon irradiation of male and female voxel models*. Phys. Med. Biol. **47**, 2367–2385 (2002)
11. Kramer, R., Viera, J. W., Khoury, H. J., and de Andrade Lima, F. *MAX meets ADAM: a dosimetric comparison between a voxel-based and a mathematical model for external exposure to photons*. Phys. Med. Biol. **49**, 887–910 (2004)
12. Liu, H., Gu, J., Caracappa, P. F. and Xu, X. G. *Comparison of two types of adult phantoms in terms of organ doses from diagnostic CT procedures*. Phys. Med. Biol. **55**, 1441–1451 (2010)
13. Lee, C., Kim, K. P., Long, D., Fisher, R., Tien, C., Simon, S. L., Bouville, A. and Bolch, W. E. *Organ doses for reference adult male and female undergoing computed tomography estimated by Monte Carlo simulations*. Med. Phys. **38**, 1196–1206 (2011)
14. Zhang, Y., Li, X., Segars, W. P. and Samei, E. *Organ doses, effective doses, and risk indices in adult CT: Comparison of four types of reference phantoms across different examination protocols*. Med. Phys. **39**, 3404–3423 (2012)
15. Kalender, W. A., Schmidt, B., Zankl, M. and Schmidt, M. *A PC program for estimating organ dose and effective dose values in computed tomography*. Eur. Radiol. **9**, 555–562 (1999)
16. Stamm, G. and Nagel, H. D. *CT-Expo - a novel program for dose evaluation in CT*. Fortschr. Röntgenstr. **174**, 1570–1576 (2002)
17. ImPACT CT patient dosimetry calculator Excel spreadsheet. Available from Imaging Performance and Assessment for Computed Tomography webpage at <http://www.impactscan.org/>
18. International Commission on Radiological Protection *Adult Reference Computational Phantoms* ICRP Publication 110, Annals ICRP **39(2)** (2009)
19. Schlattl, H., Zankl, M., Becker, J. and Hoeschen, C. *Dose conversion coefficients for CT examinations of adults with automatic tube current modulation*. Phys. Med. Biol. **55**, 2123–2145 (2010)
20. Schlattl, H., Zankl, M., Becker, J. and Hoeschen, C. *Dose conversion coefficients for paediatric CT examinations with automatic tube current modulation*. Phys. Med. Biol. **57**, 6309–6326 (2012)
21. Kawrakow, I., Mainegra-Hing, E., Rogers, D. W. O., Tessier, F. and Walters, B. R. B. *The EGSnrc Code System: Monte Carlo Simulation of Electron and Photon Transport*. NRCC Report PIRS-701 (2017)
22. Turner, A. C., Zankl, M., DeMarco, J. J., Cagnon, C. H., Zhang, D., Angel, E., Cody, D. D., Stevens, D. M., McCollough, C. H. and McNitt-Gray, M. F. *The feasibility of a scanner-independent technique to estimate organ dose from MDCT scans: Using CTDI<sub>vol</sub> to account for differences between scanners* Med. Phys. **37**, 1816–1825 (2010)
23. International Commission on Radiological Protection *2007 Recommendations of the International Commission on Radiological Protection*. ICRP Publication 103. Annals ICRP 37 (2-4), Ed. J. Valentin (2007)
24. *CIRS. ATOM Dosimetry Phantoms. Models 701-706*. Computerized Imaging Reference Systems (CIRS), Inc. Norfolk, Virginia (2012)
25. *CIRS. User Guide and Technical Information. ATOM Dosimetry Phantom. Adult Male Phantom. Model 701-D*. Computerized Imaging Reference Systems (CIRS), Inc. Norfolk, Virginia (2012)
26. European Commission. *Recommendations for patient dosimetry in diagnostic radiology using TLD* Report EUR 1964 EN (2000)
27. Lechel, U., Becker, C., Langenfeld-Jäger, G. and Brix, G. *Dose reduction by automatic exposure control in multidetector computed tomography. comparison between measurement and calculation*. Eur. Radiol. **19**, 1027–1034 (2008)

28. Nelson, W. R., Rogers, D. W. O. and Kawrakow, I. *The EGS4 Code System*. Report SLAC-265 (1985)
29. Turner, A. C., Zhang, D., Kim, H. J., DeMarco, J. J., Cagnon, C. H., Angel, E., Cody, D. D., Stevens, D. M., Primak, A. N., McCollough, C. H. et al. *A method to generate equivalent energy spectra and filtration models based on measurement for multidetector CT Monte Carlo dosimetry simulations*. *Med. Phys.* **36**, 2154–2164 (2009)
30. Boone, J. M. *Method for evaluating bow tie filter angle-dependent attenuation in CT: Theory and simulation results*. *Med. Phys.* **37**, 40–48 (2010)
31. Poludniowski, G., Landry, G., DeBlois, F., Evans, P. M. and Verhaegen, F. *SpekCalc: a program to calculate photon spectra from tungsten anode x-ray tubes*. *Phys. Med. Biol.* **54**, N433–N438 (2009)
32. International Commission on Radiological Protection *Reference Man: Anatomical, Physiological and Metabolic Characteristics*. ICRP Publication 23 (1974)
33. Zankl, M., Panzer, W. and Drexler, G. *The calculation of dose from external photon exposures using reference human phantoms and Monte Carlo methods: Part IV. Organ Doses from Computed Tomographic Examinations*. GSF Report **30/91** (1999)
34. Schlattl, H., Zankl, M. and Petoussi-Hens, N. *Dose conversion coefficients for voxel models of the reference male and female from idealized photon exposure*. *Phys. Med. Biol.* **52**, 6243–6261 (2007)